

Increasing Accuracy of Kalman Filter-based Sensorless Control of Wind Turbine PM Synchronous Generator

Tomislav Lončarek, Vinko Lešić, Mario Vašak

Faculty of Electrical Engineering and Computing, University of Zagreb, Zagreb, Croatia
tomislav.loncarek@fer.hr vinko.lesic@fer.hr mario.vasak@fer.hr

Abstract—Wind turbines require periodic maintenance procedures to ensure reliable operation of the system. Regular servicing of the rotor demands calibration of the speed and position sensor in aggravated circumstances of the dynamic wind. This sensor is one of the most critical components for the drive reliability and the calibration greatly increases the time of repair. The main focus of the paper is to eliminate the need for encoder mounted on the generator shaft in wind turbine applications by implementing an algorithm for speed and flux position estimation. Two unscented Kalman filters are used in a dual configuration to ensure both robust and accurate control performance under the variable wind conditions. The estimation algorithm is comprised of stationary frame model-based observer for enabling robust speed estimation, superposed with rotor flux frame model-based observer for fine accuracy tuning of the flux position needed for generator field-oriented control. Experimental results obtained on a scaled laboratory setup show that presented method performs well with improved accuracy of speed and flux position estimation, and ensures smooth performance of sensorless generator control.

Index Terms—Permanent Magnet Synchronous Generator, Sensorless Control, Unscented Kalman Filter, Flux Position Estimation.

I. INTRODUCTION

In recent years, wind turbines (WTs) are becoming a promising alternative to electrical energy generation by fossil or nuclear power plants. They however experience reliability issues due to remote locations and stochastic wind character, and a lot of effort is put into increasing their market competence.

Permanent magnet synchronous generator (PMSG) has become a hot research topic in the field of WT generators due to its advantages such as high power density, high efficiency, high reliability and high dynamic performance [1]. As a high performance control scheme, field-oriented control (FOC) is widely used in electrical machines and WT generators. In most applications, both rotor speed and position are determined using absolute encoders, with performance level proportional to its cost. Utilization of a high-precision complex encoder in a harsh environment certainly increases cost and decreases reliability. Moreover, frequent maintenance interventions require time-consuming encoder calibrations, which are possible to be performed only in weak and steady wind circumstances. Therefore, sensorless generator control in WT applications has drawn attention of many researches.

Closed-loop observers used for this purpose differ with respect to accuracy, robustness, and sensitivity against model parameter variations. Methods of speed and flux position estimation in electrical machines and PMSG can be divided into two groups: methods based on mathematical model and so-called injection estimators. The main drawback of model-based estimators is insufficient performance at low speed. Injection estimators introduce a high frequency signal (voltage or current) injected into the generator and the flux position and speed are then determined by processing the resulting currents or voltages [2], [3].

In the paper we opt for unscented Kalman filter (UKF), an optimal recursive algorithm suitable to estimate the state of nonlinear dynamic systems [4]. There are several researches and applications of UKF to PMSG sensorless control. Corresponding publications indicate convergence problems at startup by using the PMSG model in (α, β) stationary frame and constant error in the flux position estimation by using the PMSG model in rotating (d, q) frame [5]–[7].

Precisely determined flux position, generator speed and stator currents in (d, q) rotating frame are important for implementation of FOC. This paper investigates an improved state observer by using two UKFs with different combined models of PMSG. In the proposed observer design, the first UKF estimates flux position and generator speed in (α, β) frame based on machine physics and salient rotor poles, and then the second UKF reduces the flux position error and accurately estimates stator currents in rotating (d, q) frame needed for FOC. Behavior of the proposed estimator and developed sensorless control of PMSG is analyzed by simulation and experimental results for a 700 kW variable-speed variable-pitch wind turbine model with a 5.2 kW PMSG scaled to match the torque and power of a 700 kW machine. Obtained results show that the proposed observer design provides improved performance over wide speed ranges i.e., both low and high speeds. Furthermore, start-up procedure is not required since the physical pole position is estimated as well.

This paper is organized as follows. Wind turbine control system is briefly described in Section II. Mathematical models of PMSG are presented in Section III. Section IV describes the UKF algorithm. In Section V, derived observers for speed sensorless FOC are described. Section VI provides experimental results. Conclusions are drawn in Section VII.

II. WIND TURBINE SYSTEM

Direct-drive wind turbine concept with PMSG and power converter is shown in Fig. 1. Such a concept is attractive mainly because of its low maintenance cost, complete decoupling from grid, and wide range control capabilities [1].

The wind generates aerodynamical torque on the turbine that is further passed through the drive-train to the generator rotor shaft. The generator produces electrical torque and the difference between the aerodynamical torque from the wind turbine and electrical torque from the generator determines whether the mechanical system accelerates, decelerates or remains at constant speed. The generator is connected to a three-phase inverter that rectifies the current from the generator to charge a DC-link capacitor. The DC-link feeds a second three-phase inverter that finally exports produced power to the grid.

A. Wind Turbine Control System

Based on the WT aerodynamical behavior, the turbine catches only a part of the kinetic energy contained in the wind:

$$P_t = \frac{1}{2} \rho_{air} R_r^2 \pi C_P(\lambda, \beta) v^3, \quad (1)$$

where P_t is the power captured by the rotor, R_r is the rotor radius, ρ_{air} is the air density and v is the speed of the wind. The amount of the useful power is defined by the power coefficient C_p , which, for a given WT rotor, depends on the pitch angle of rotor blades β and on the tip-speed-ratio λ defined as:

$$\lambda = \frac{\omega \cdot R_r}{v}, \quad (2)$$

where ω is the rotational speed of the rotor. Aerodynamical characteristics of the rotor are represented by the C_p - λ relation. Power coefficient C_p has a maximum value for an optimal tip-speed-ratio value λ_{opt} and thus, the power extracted by wind rotor is maximized for any wind speed.

Aerodynamic torque T_t of a wind turbine rotor can be obtained from (1) as follows:

$$T_t = \frac{P_t}{\omega} = \frac{1}{2} \rho_{air} R_r^3 \pi C_T(\lambda, \beta) v^2, \quad (3)$$

where $C_T = C_P/\lambda$ is the torque coefficient.

Below rated speed operation, torque control loop adjusts the generator torque to achieve desired WT rotational speed in order to provide the optimum power production. In above

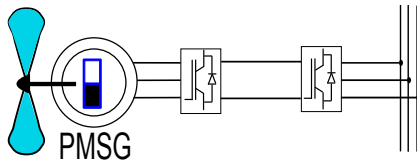


Fig. 1. General concept of a wind turbine system with PMSG.

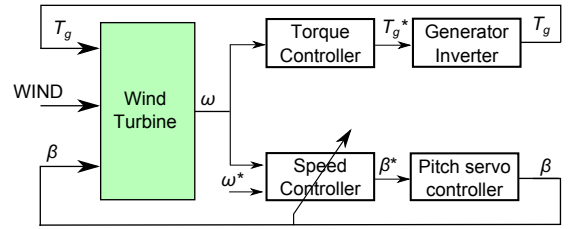


Fig. 2. Control system of a variable-speed variable-pitch wind turbine.

rated speed operation, the power output is maintained constant while reducing the aerodynamic torque and keeping generator speed at the rated value. For this task, the pitch control loop is responsible. Both control loops are shown in Fig. 2.

III. MATHEMATICAL MODEL OF PMSG

The PMSG model can be derived in the stationary (α, β) reference frame, fixed to the stator, or in the synchronous (d, q) reference frame that rotates aligned with the rotor flux.

A. Mathematical model of PMSG in (d, q) reference frame

In rotating (d, q) reference frame linked to a rotor flux, the PMSG is described with DC voltages and currents. This enables independent torque and flux control, i.e., the FOC. Equations for the d -axis and q -axis currents are:

$$\begin{aligned} \frac{di_d}{dt} &= \frac{1}{L_d} (u_d - R_s i_d + \Delta u_d), \\ \frac{di_q}{dt} &= \frac{1}{L_q} (u_q - R_s i_q + \Delta u_q), \end{aligned} \quad (4)$$

with decoupling voltages Δu_d , Δu_q :

$$\begin{aligned} \Delta u_d &= L_q \omega_e i_q, \\ \Delta u_q &= -L_d \omega_e i_d - \psi_{pm} \omega_e, \end{aligned} \quad (5)$$

where u_d and u_q are the d -axis and q -axis voltages, ω_e is rotor flux speed, L_d and L_q are generator inductances in d -axis and q -axis, ψ_{pm} is permanent magnet flux and R_s is stator resistance.

B. Mathematical model of PMSG in (α, β) reference frame

The PMSG voltage and flux linkage equations in stationary (α, β) reference frame are:

$$\begin{aligned} u_\alpha &= R_s i_\alpha + \frac{d}{dt} \psi_\alpha, \\ u_\beta &= R_s i_\beta + \frac{d}{dt} \psi_\beta, \end{aligned} \quad (6)$$

$$\psi_\alpha = (L_a + L_b \cos 2\rho) i_\alpha + i_\beta L_b \sin 2\rho + \psi_{pm} \cos \rho, \quad (7)$$

$$\psi_\beta = L_b \sin 2\rho i_\alpha + (L_a - L_b \cos 2\rho) i_\beta + \psi_{pm} \sin \rho,$$

where $L_a = (L_d + L_q)/2$ and $L_b = (L_d - L_q)/2$. Voltages, currents and the stator flux linkage in the α -axis and the β -axis are (u_α, u_β) , (i_α, i_β) and $(\psi_\alpha, \psi_\beta)$, respectively. Variable ρ is the flux position with respect to the stationary frame.

IV. UNSCENTED KALMAN FILTER ALGORITHM

As UKF approximates the probability distribution of a nonlinear function rather than the first-order linearization of the function itself, it uses a deterministic sampling approach to capture the mean and covariance of estimates with a minimal set of sample points, called sigma points [4]. Each sigma point is put through nonlinear model dynamics and outputs are weighted to obtain mean and covariance of the state prediction. Measurements are finally used to correct the prediction and obtain estimated values. In the sequel, UKF equations are presented.

General discrete nonlinear system is given with:

$$\mathbf{x}_k = F(\mathbf{x}_{k-1}, \mathbf{u}_{k-1}, \mathbf{v}_{k-1}), \quad (8)$$

$$\mathbf{y}_k = H(\mathbf{x}_k, \mathbf{n}_k), \quad (9)$$

where $\mathbf{x}_k \in \mathbb{R}^n$ is the state vector, $\mathbf{y}_k \in \mathbb{R}^m$ is the output vector. Vectors $\mathbf{v}_k \in \mathbb{R}^n$ and $\mathbf{n}_k \in \mathbb{R}^m$ are process noise and measurement noise, respectively.

State vector \mathbf{x}_k^a in a discrete time-instant k is augmented to include \mathbf{v} and \mathbf{n} :

$$\mathbf{x}_k^a = [\mathbf{x}_k^T \quad \mathbf{v}_k^T \quad \mathbf{n}_k^T]^T.$$

With respect to the system (8) and (9), the UKF estimation can be expressed as:

Initialization

$$\begin{aligned} \hat{\mathbf{x}}_0 &= \mathbb{E}[\mathbf{x}_0], \\ \mathbf{P}_0 &= \mathbb{E}[(\mathbf{x}_0 - \hat{\mathbf{x}}_0)(\mathbf{x}_0 - \hat{\mathbf{x}}_0)^T], \\ \hat{\mathbf{x}}_0^a &= \mathbb{E}[\mathbf{x}^a] = [\hat{\mathbf{x}}_0^T \quad \mathbf{0} \quad \mathbf{0}]^T, \\ \mathbf{P}_0^a &= \mathbb{E}((x_0^a - \hat{x}_0^a)^T(x_0^a - \hat{x}_0^a)) = \begin{bmatrix} \mathbf{P}_0 & \mathbf{0} & \mathbf{0} \\ \mathbf{0} & \mathbf{Q} & \mathbf{0} \\ \mathbf{0} & \mathbf{0} & \mathbf{R} \end{bmatrix}, \end{aligned} \quad (10)$$

Sigma points calculation and time update

$$\chi_{k-1}^a = \left[\hat{\mathbf{x}}_{k-1}^a \quad \hat{\mathbf{x}}_{k-1}^a + \gamma \sqrt{\mathbf{P}_{k-1}^a} \quad \hat{\mathbf{x}}_{k-1}^a - \gamma \sqrt{\mathbf{P}_{k-1}^a} \right], \quad (11)$$

$$\chi_{k|k-1}^x = \mathbf{F}(\chi_{k-1}^x, u_{k-1}, \chi_{k-1}^v), \quad (12)$$

$$\hat{\mathbf{x}}_k^- = \sum_{i=0}^{2L} W_i^{(m)} \chi_{i,k|k-1}^x, \quad (13)$$

$$\mathbf{P}_k^- = \sum_{i=0}^{2L} W_i^{(c)} [\chi_{i,k|k-1}^x - \hat{\mathbf{x}}_k^-] [\chi_{i,k|k-1}^x - \hat{\mathbf{x}}_k^-]^T, \quad (14)$$

$$\Upsilon_{k|k-1} = \mathbf{H}(\chi_{k|k-1}^x, \chi_{k-1}^n), \quad (15)$$

$$\hat{\mathbf{y}}_k^- = \sum_{i=0}^{2L} W_i^{(m)} \Upsilon_{i,k|k-1}, \quad (16)$$

where

$$\begin{aligned} W_0^{(m)} &= \frac{\lambda_{ut}}{(L + \lambda_{ut})}, \\ W_0^{(c)} &= \frac{\lambda_{ut}}{(L + \lambda_{ut})} + (1 - \alpha^2 + \beta), \\ W_i^{(m)} &= W_i^{(c)} = \frac{\lambda_{ut}}{2(L + \lambda_{ut})}, \quad i = 1, \dots, 2L, \\ \lambda_{ut} &= \alpha^2(L + \kappa) - L. \end{aligned} \quad (17)$$

Measurement update

$$\mathbf{P}_{\hat{y}_k^-, \hat{y}_k^-} = \sum_{i=0}^{2L} W_i^{(c)} [\Upsilon_{i,k|k-1} - \hat{\mathbf{y}}_k^-] [\Upsilon_{i,k|k-1} - \hat{\mathbf{y}}_k^-]^T, \quad (18)$$

$$\mathbf{P}_{x_k^-, y_k^-} = \sum_{i=0}^{2L} W_i^{(c)} [\chi_{i,k|k-1}^x - \hat{\mathbf{x}}_k^-] [\Upsilon_{i,k|k-1} - \hat{\mathbf{y}}_k^-]^T, \quad (19)$$

$$K_k = \mathbf{P}_{x_k^-, y_k^-} \mathbf{P}_{\hat{y}_k^-, \hat{y}_k^-}^{-1}, \quad (20)$$

$$\hat{\mathbf{x}}_k = \hat{\mathbf{x}}_k^- + K_k (\mathbf{y}_k - \hat{\mathbf{y}}_k^-), \quad (21)$$

$$\mathbf{P}_k = \mathbf{P}_k^- - K_k \mathbf{P}_{\hat{y}_k^-, \hat{y}_k^-} K_k^T. \quad (22)$$

Parameters W_i are scalar weights, L is the state dimension. The parameter α determines the spread of the sigma points around $\hat{\mathbf{x}}$ and is usually set to $10^{-4} \leq \alpha \leq 1$. For Gaussian distributions β is usually set to $\beta = 2$. Process and measurement noise covariances are \mathbf{Q} and \mathbf{R} , respectively. More information about UKF can be found in [4].

V. OBSERVER DESIGN

This section describes on-line estimation process of FOC variables, speed and flux position by using two UKFs with two combined models of PMSG. In this approach, two filters are implemented in a so-called dual configuration form, one for rotor speed ω_g , flux angle position ρ and currents in stationary frame (i_α, i_β), and another for fine tuning of the flux position ϵ and currents in rotating (d, q) frame. Figure 3 shows block diagram of the estimation circuit and control system.

Disadvantage of using the PMSG model in rotating (d, q) frame is that stator and rotor poles need to be aligned at the generator start-up. Otherwise L_d and L_q have wrong values and FOC operates with erroneous decoupling procedure, which results in model discrepancy and wrong current and torque values, as presented in Fig. 4. Tuning of a filter with (α, β) model is very demanding and uncertain as the process covariance matrix is dependent on the operating point.

Initial alignment of stator and rotor poles is usually achieved by applying DC current through the stator windings. However, in WT applications and high wind speeds, even the aerodynamical brake position of blades and rated stator current value may not suffice to steadily align the poles. The system must therefore wait for weak winds to initialize the algorithm. The same problem occurs with encoder calibration. Another disadvantage of the (d, q) model is that speed sensorless and corresponding flux position estimation performs well only in higher speeds when back electromotive force (ω_e) is considerable.

Advantage of (α, β) model lies in accurate speed estimation for sensorless control, suitable for both low and high speeds as the model is tied with machine physics and salient poles, [8]. However, the (α, β) estimator needs to be tuned for larger

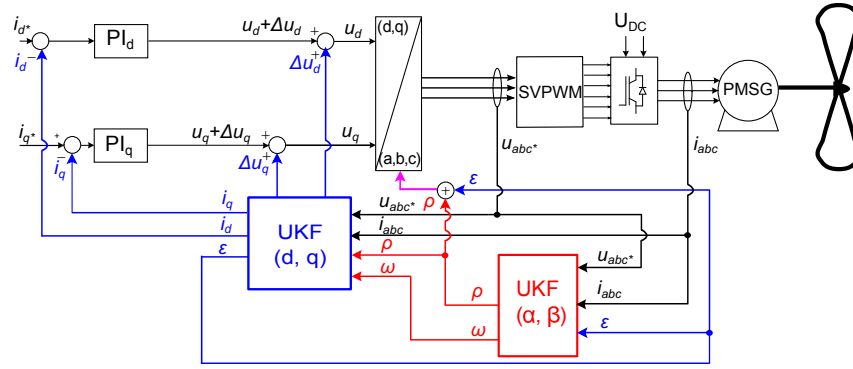


Fig. 3. Derived robust and accurate speed and flux position observer implemented in dual UKF configuration.

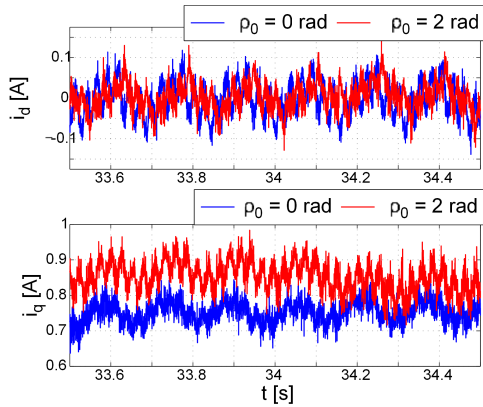


Fig. 4. Estimation of currents with (d, q) model for aligned and misaligned starting pole positions (experimental result).

uncertainty as it is used for estimation of sinusoidal variables. This also introduces unsteady and high-uncertainty control variables that reduces the control performance if the filter is poorly tuned, as shown in Fig. 5.

On the other hand, (d, q) model shows outstanding capability in extraction of fundamental current components and smooth FOC performance with speed measurements [9]. Two

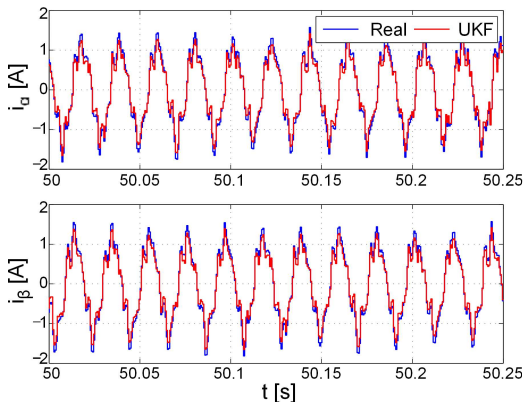


Fig. 5. Poor current estimation performance and distortion with (α, β) model due to inadequate filter tuning (experimental result).

models are therefore used in combination to extract advantages of both while compensating the disadvantages at the same time. Therefore the (α, β) observer is used for robust speed estimation and sensorless operation while (d, q) observer is further on used for fundamental components extraction and fine tuning of flux position estimation. Both observers are implemented by using UKF algorithms and are put in the dual filter configuration (Fig. 3), where each of the filters uses the most recent information from another one. An example of dual filter configuration is a so-called braided filter well known in electrical drives community [6].

In UKF with (d, q) model state vector is $\mathbf{x} = [i_d \ i_q \ \epsilon]$, input vector is $\mathbf{u} = [u_a \ u_b \ \rho \ \omega_e]$, where the measurement of phase voltages is replaced by the reference space-vector pulse width modulation (SVPWM) signals, output vector is $\mathbf{y} = [i_d \ i_q \ \epsilon]$. Vector function $\mathbf{F}(\cdot)$ is defined with equations (4) and (5), and flux position correction ϵ is regarded as constant

$$\frac{d\epsilon}{dt} = 0. \quad (23)$$

Output vector function $\mathbf{H}(\cdot)$ is given with:

$$\begin{aligned} i_a &= i_{sd} \cos(\rho + \epsilon) - i_{sq} \sin(\rho + \epsilon), \\ i_b &= \frac{1}{2}(\sqrt{3}i_{sq} - i_{sd}) \cos(\rho + \epsilon) + \frac{1}{2}(\sqrt{3}i_{sd} - i_{sq}) \sin(\rho + \epsilon). \end{aligned} \quad (24)$$

In UKF with (α, β) model state vector is $\mathbf{x} = [i_\alpha \ i_\beta \ \rho \ \omega_e]$, input vector is $\mathbf{u} = [u_a \ u_b \ \epsilon]$, where measurement of the phase voltages is, also, replaced by the reference (SVPWM) signals, output vector is $\mathbf{y} = [\rho \ \omega_e]$. Vector function $\mathbf{F}(\cdot)$ is derived by substituting (7) into (6), and supplemented with equations:

$$\frac{d\rho}{dt} = p \cdot \omega, \quad \frac{d\omega}{dt} = 0. \quad (25)$$

Output vector function $\mathbf{H}(\cdot)$ is given with inverse Clark's transformation, defined as:

$$i_a = i_\alpha, \quad i_b = -\frac{1}{2}i_\alpha + \frac{\sqrt{3}}{2}i_\beta. \quad (26)$$

In vector function $\mathbf{F}(\cdot)$ instead of ρ it is used $\rho + \epsilon$, both in (d, q) and (α, β) models. Because the electrical system time constant is much smaller than the mechanical time constant, in UKF for estimation of flux position and rotor speed based on PMSG

model in stationary (α, β) frame, rotor speed is regarded as constant within the sampling time step T_s . Thus the uncertain mechanical parameters (moment of inertia and load torque) are not required. In both UKFs, a 4th order Runge-Kutta numerical integration algorithm is applied to PMSG model equations for obtaining state values at the next time step.

A. Simulation results

Developed system is verified first by using Matlab/Simulink and Plexim/PLECS, a professional simulation platform for power electronics systems. Parameters used in simulations are given in Tab. I.

Simulation results, presented in Fig. 6 and Fig. 7, show that estimated values have fast convergence to ideal values for both UKFs and that proposed observer design can be efficiently implemented on laboratory setup.

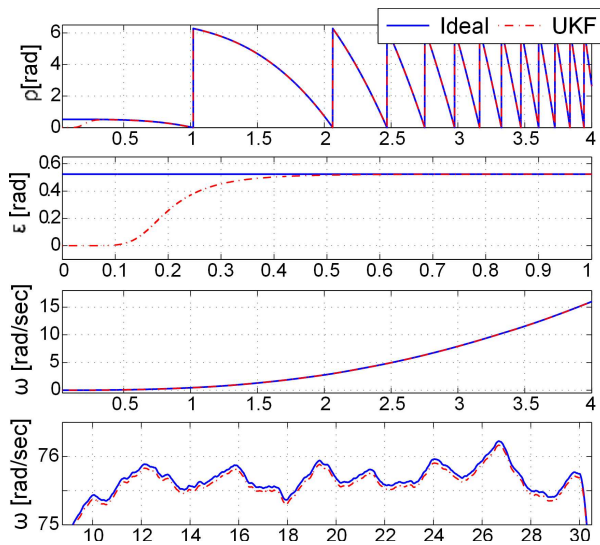


Fig. 6. Estimated flux position ρ , flux position correction ϵ and rotor speed ω .

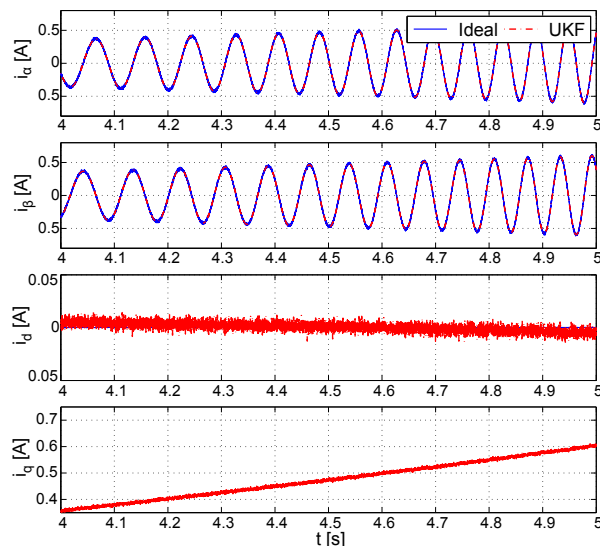


Fig. 7. Estimated currents in (α, β) and (d, q) frame.

VI. EXPERIMENTAL RESULTS

The experimental setup consists of three main parts: wind turbine emulator, that acts as WT aerodynamics, the PMSG that converts mechanical energy to electrical energy and the breaking resistor on which generated electrical power is dissipated.

Generator with parameters from Tab. I is supplied with three-phase voltage pulses from a Danfoss FC302 converter. The FC302 is a standard IGBT-VS inverter where the original control card is replaced to enable desired IGBT switching, controlled by a dSPACE DS1103 digital controller. Measurements of the DC voltage, currents and voltages are obtained with LEM sensors.

TABLE I
PMSG AND WT PARAMETERS

Description	Parameter	Value
P_{gn}	Rated power	5.2 kW
I_n	Rated current	11 A
p	number of pole pairs	4
ω_n	Rated rotor speed	2000 r/min
R_s	Rotor resistance	0.288 Ω
L_d	Direct-axis inductance	7.9 mH
L_q	Quadrature-axis inductance	7.9 mH
ψ_{pm}	Permanent magnet flux	0.3788 mH
P_n	Rated WT power	700 kW
ω_n	Rated WT rotor speed	3.037 rad/s
C_{Pmax}	Rated WT torque	0.4745
λ_{opt}	Optimal tip-speed-ratio	7.4
R	Radius of WT rotor	25 m
h_{tower}	Tower height	50 m

The digital controller is also used for hardware in the loop simulation of the 700 kW wind turbine aerodynamics with parameters from Table I. Wind turbine parameters are adapted to laboratory setup by speed and power scaling coefficients: $n_s = \omega_{gn}/\omega_n$ and $n_t = P_{gn}/P_n$. The turbine emulation is implemented with a squirrel-cage induction motor and Danfoss FC302 frequency inverter that receives stochastic and realistic aerodynamic torque reference from the control platform.

As shown in Fig. 8, estimated rotor speed ω and flux position ρ track the real values with good precision at startup and during variable wind speed condition. Rotor speed measurement is only used for comparison and FOC is operating in sensorless mode.

Stator currents estimation also gives a good tracking performance, as shown in Fig. 9. Real and estimated currents in rotating (d, q) frame contain a small fluctuation because of the flux saturation, which is attenuated with UKF and fundamental components are extracted and used in FOC. Estimated currents are suitable for FOC implementation. Fig. 10 shows estimation errors of results shown in Fig. 8. Such large transients are given to illustrate dynamical performance of the proposed method, but are not a realistic case since real WTs attenuate them with very large moment of inertia.

Covariance matrix elements of the state process noise in UKF based on PMSG model in (α, β) frame and UKF based on PMSG model in (d, q) are chosen as:

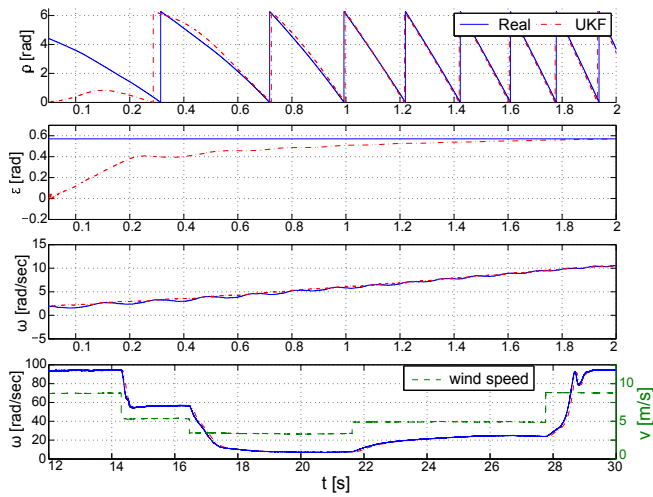


Fig. 8. Estimation of flux position ρ , flux position correction ϵ and rotor speed ω .

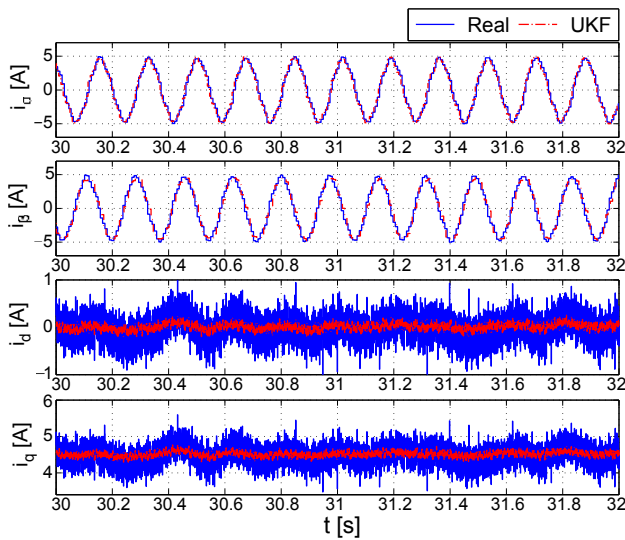


Fig. 9. Estimated currents in (α, β) and (d, q) frame.

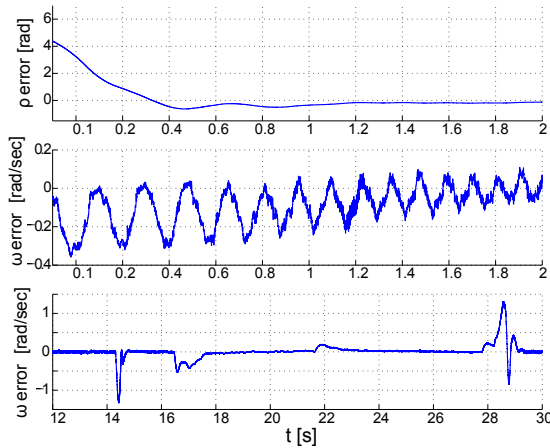


Fig. 10. Errors between estimated and measured flux position ρ and rotor speed ω .

$$\mathbf{Q}_{(\alpha,\beta)} = \text{diag}([0.05, 0.05, 5 \cdot 10^{-5}, 5 \cdot 10^{-4}]),$$

$$\mathbf{Q}_{(d,q)} = \text{diag}([0.05, 0.005, 5 \cdot 10^{-9}]).$$

Initial values of covariance matrices $\mathbf{P}_0(\alpha,\beta)$ and $\mathbf{P}_0(d,q)$ are:

$$\mathbf{P}_0(\alpha,\beta) = \text{diag}([0.05, 0.05, 0.005, 0.005]),$$

$$\mathbf{P}_0(d,q) = \text{diag}([0.05, 0.005, 0.1]).$$

Measurement noise covariance matrices in both UKF:

$$\mathbf{R}_{(\alpha,\beta),(d,q)} = \text{diag}([0.01, 0.01]).$$

Since WT generator is starting from standstill condition, the initial state vector \mathbf{x}_0^a in both UKFs is considered as a null vector. Presented approach with dual UKF is also far easier to tune than sole (α, β) observer and thus is a more robust solution.

VII. CONCLUSIONS

In this paper, a dual Unscented Kalman filter observer is developed for estimation of stator currents, flux position and rotor speed that are further employed for achieving the sensorless field-oriented control of permanent-magnet synchronous generator. Simulation and experimental results show that the designed estimator achieves improved accuracy and robustness of estimated variables in both low-speed and high-speed regimes. The developed observer can be also adapted for the case of induction generators or small electrical motor applications and corresponding sensorless control techniques.

ACKNOWLEDGEMENT

The research leading to these results has received funding from the "Centre of Excellence for Structural Health" (CEEStructHealth) supported by the European Union under contract IPA2007/HR/16IPO/001-040513.

REFERENCES

- [1] H. Tiegna, Y. Amara, G. Barakat, B. Dakyo, "Overview of high power turbine generators", *ICRERA Renewable Energy Research and Applications*, pp. 1–6, Nov. 2012.
- [2] M. Pacas, "Sensorless Drives in Industrial Applications", *IEEE Industrial Electronics Magazine* vol. 5, no. 2, pp. 16–23, Jun. 2011.
- [3] J. Holtz, "Sensorless Control of Induction Machines - With or Without Signal Injection?", *IEEE Transactions on Industrial Electronics* vol. 53, no. 21, Feb. 2006.
- [4] S. Julier, J. Uhlmann, H.F. Durrant-White, "A new method for nonlinear transformation of means and covariances in filters and estimators," *IEEE Trans. Automatic Control*, vol. 45, no. 3, pp. 477–482, Mar. 2000.
- [5] T. F. Chan, P. Borsje, W. Wang, "Application of Unscented Kalman filter to sensorless permanent-magnet synchronous motor drive", *IEEE International Electric Machines and Drives Conference*, pp. 631–638, May 2009.
- [6] S. Bogosyan, M. Barut, M. Gokasan, "Experimental Evaluation of Braided EKF for Sensorless Control of Induction Motors", *IEEE Transactions on Industrial Electronics*, vol. 55, pp. 620–632, Feb. 2008.
- [7] G. Rigatos, P. Siano, N. Zervos, "Sensorless Control of Distributed Power Generators With the Derivative-Free Nonlinear Kalman Filter", *IEEE Transactions on Industrial Electronics*, vol. 61, pp. 6369–6382, Jan. 2014.
- [8] S. Bolognani, S. Calligaro, R. Petrella, "Sensorless control for IPMSM using PWM excitation: Analytical developments and implementation issues," *Symposium on Sensorless Control for Electrical Drives (SLED)*, 2011, pp. 64–73, Sept. 2011.
- [9] C. Busca, A.-I. Stan, T. Stanciu, D.I. Stroe, "Control of Permanent Magnet Synchronous Generator for large wind turbines", *IEEE International Symposium on Industrial Electronics*, vol. 1, pp. 3871–3876, Jul. 2010.